

Lifetime prediction of optocouplers in digital input and output modules based on bayesian tracking approaches

Insun Shin¹ and Daeil Kwon^{*2}

¹Department of System Design and Control Engineering, Ulsan National Institute of Science and Technology, Ulsan, 44919, Republic of Korea

²School of Mechanical, Aerospace and Nuclear Engineering, Ulsan National Institute of Science and Technology, Ulsan, 44919, Republic of Korea

(Received May 8, 2017, Revised March 15, 2018, Accepted March 19, 2018)

Abstract. Digital input and output modules are widely used to connect digital sensors and actuators to automation systems. Digital I/O modules provide flexible connectivity extension to numerous sensors and actuators and protect systems from high voltages and currents by isolation. Components in digital I/O modules are inevitably affected by operating and environmental conditions, such as high voltage, high current, high temperature, and temperature cycling. Because digital I/O modules transfer signals or isolate the systems from unexpected voltage and current transients, their failures may result in signal transmission failures and damages to sensitive circuitry leading to system malfunction and system shutdown. In this study, the lifetime of optocouplers, one of the critical components in digital I/O modules, was predicted using Bayesian tracking approaches. Accelerated degradation tests were conducted for collecting the critical performance parameter of optocouplers, current transfer ratio (CTR), during their lifetime. Bayesian tracking approaches, including extended Kalman filter and particle filter, were applied to predict the failure. The performance of each prognostic algorithm was then compared using accuracy and robustness-based performance metrics.

Keywords: digital input and output modules; optocouplers; lifetime prediction; particle filter; extended Kalman filter Bayesian tracking approaches

1. Introduction

Digital input and output (digital I/O) modules are widely used to connect digital sensors and actuators to automation systems. Digital I/O modules provide flexible connectivity extension to numerous sensors and actuators. Furthermore, digital I/O modules protect measurement and control systems from high voltages and currents by isolation (National Instruments, 2015). Under the growing automation system complexity, the number of digital I/O modules is rapidly increasing along with the number of sensors and actuators. Typical sensors include proximity, flow, pressure, and temperature sensors. Actuators can be solenoid valves, motors, and pumps. Fig. 1 shows an example of digital I/O module connection in a measurement and control system.

Digital I/O modules typically consist of resistors, electrolytic capacitors, optocouplers, and protocol processors for transmitting digital signals. The components are inevitably affected by operating and environmental stress conditions, such as high voltage, high current, high temperature, and temperature cycling. Stress conditions may cause performance degradation of the components, and eventually lead to failures of digital I/O modules. Because

digital I/O modules transmit signals or isolate the systems from unexpected voltage and current transients, their failures may result in signal transmission failures and damages to sensitive circuitry leading to system malfunction. Reliability assessment and lifetime prediction of digital I/O modules is required to protect modules from unexpected failures resulting in automation system downtime.

Reliability of digital systems, inclusive of digital I/O modules, has been studied by many researchers in a view of dynamic interaction between electronic components. Digital system malfunctions are critical in the nuclear industry because failures of a digital system could lead to catastrophic disasters, as well as damage to nuclear power plants. Thus, many researchers have focused on evaluating the reliability of digital systems in nuclear power plants. The U.S. nuclear regulatory commission (Chu *et al.* 2008) proposed a conventional probabilistic safety assessment (PSA) method to model the common causes of failure related to digital system components. PSA methods were applied to model the reliability of digital systems for feedwater control (Chu *et al.* 2009) and nuclear safety-related digital instrumentation and control systems (Authen and Holmberg 2012, Chu *et al.* 2008, Lee *et al.* 2016). In addition to the traditional reliability modeling approaches, it has emerged to assess the reliability by predicting the lifetime for predictive maintenance. Predictive maintenance prevents system failures through estimating the remaining useful life based on system health monitoring and failure

*Corresponding author, Ph.D.
E-mail: dkwon@unist.ac.kr

prognosis, thereby reducing unexpected system downtime and downtime costs.

One method for predictive maintenance is to identify the critical components at high risk of failures, and to predict the critical component lifetime. A digital I/O module consists of approximately 60 components in charge of power conversion, signal isolation, signal transformation, and communication protocol processing. According to IEEE Standard 650 (IEEE Standards Association, 2006), communication protocol processors, electrolytic capacitors, optocouplers, and surge killers often experience wear out failures in a digital I/O module. Their potential failure mechanisms of the critical components were surveyed as shown in Table 1. A dominant failure mechanism of digital I/O modules in use condition is distortion and signal loss in optocouplers due to high temperature and high current (Slama *et al.* 2008, Shi *et al.* 2014). High temperature and high current induce electromigration in light emitting diodes (LEDs) used as a light source. Electromigration continuously reduces the LED light intensity. Intensity reduction of an LED light causes signal distortion and reduction. The performance of an optocoupler degrades over time due to LED wear-out damage, which can eventually cause digital I/O module failure.

The purpose of this paper is to predict the lifetime of optocouplers using Bayesian tracking approaches by monitoring the performance degradation of optocouplers. This study performs accelerated degradation tests (ADTs) of optocouplers to obtain degradation data for predicting the lifetime of optocouplers. The lifetime of optocouplers is predicted using Bayesian tracking algorithms, EKF and PF, which are representative algorithms applicable to nonlinear system models. Finally, the prognostic performance of each algorithm was evaluated by accuracy and robustness-based performance metrics.

2. Bayesian tracking approaches

Bayesian tracking approaches have widely been used to predict the evolution of system damage.

Table 1 Failure modes and causes of main functional components in a digital I/O module

Component	Failure mode	Failure cause
Communication protocol processor, EtherCAT BGA (Chiu <i>et al.</i> 2004)	Solder joint crack	Temperature cycling
	Die crack	Temperature cycling, vibration, bending
Electrolytic capacitor (Kulkarni <i>et al.</i> 2009)	Capacitance reduction	High voltage, ripple current, high temperature
	Crack	High temperature, high current
Optocoupler (Slama <i>et al.</i> 2008)	Signal distortions and reductions	High temperature, high current
	Signal velocity delay	High current
Surge protector (Brown 2004)	Resistance increment	High current
	Crack	Temperature cycling,

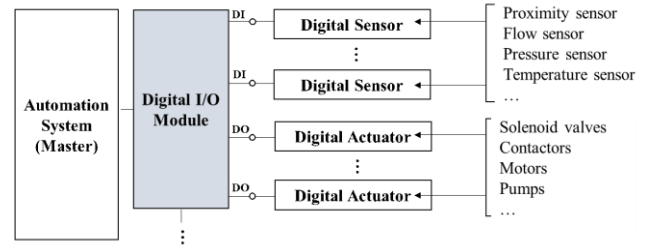


Fig. 1 And example of digital I/O module connection

Bayesian tracking-based algorithms estimate the true states of a dynamic system under the Markov assumption by employing a state dynamic model and a measurement model. Extended Kalman Filter (EKF) and particle Filter (PF) are widely used recursive Bayesian estimation techniques for solving non-linear state estimation problems (Feng *et al.* 2011, Doucet *et al.* 2001, Yoshida and Akiyama 2013, Ginsberg *et al.* 2018).

These Bayesian algorithms incorporate observations into a priori state estimate by considering the likelihood of measured values based on Bayes theorem, as shown in Eq. (1).

$$P(H|D) \propto P(D|H)P(H) \quad (1)$$

where $P(H|D)$ is the posterior probability of a hypothesis and $P(D|H)$ is the likelihood. $P(H)$ is the prior probability of a hypothesis without any evidence from measurement data. Bayes theorem computes the probability of an output, H , given measurements, D .

In non-linear state estimation problems, the evolution of the state x is under investigation. The sequence of state x can be given by the following state model

$$x_k = f_k(x_{k-1}, v_{k-1}) \quad (2)$$

where f_k is a system model associated with the state, x_{k-1} , process noise, v_{k-1} ; and k is the sequence. The state can be estimated and tracked by observations z

$$z_k = h_k(x_k, n_k) \quad (3)$$

where h_k is a measurement model, and n_k is a measurement noise. The tracking objective is to seek the estimates of the state x_k based on Bayesian perspective. The maximum a posteriori estimator (MAP) finds the value of x which maximizes the posterior distribution. Recursive Bayesian estimation including EKF and PF is the extension of MAP to time sequence estimation based of observations at each time step with the Bayes theorem and conditional independence assumption of measurements.

EKF estimates nonlinear system states using differentiable functions of state transition and measurement models. EKF expands the system model f_k and the measurement model h_k in Taylor series, and approximates the posterior probability. EKF has been applied to fault prognosis of many systems because of the applicability to nonlinear state estimation. For example, EKF was used to track the evolution of bearing faults, and to predict the remaining useful life (RUL) of bearing faults under

different operating conditions (Singleton *et al.* 2015). Failure prognosis using EKF was also applied to estimate plastic strain of ball grid array (BGA) interconnects (Lall *et al.* 2011). EKF is to find the mean and covariance of the hidden states using all the observations at a given time. The recursive process of EKF estimation consists of prediction and update, using measurements and Kalman gain. More detailed process of the EKF algorithm is presented in Algorithm 1.

Algorithm 1 The Extended Kalman filter algorithm

1. Initialization

Set initial state and covariance, x_0 and P_0

2. Iteration: for t in 1 to T

1) Prediction step

Predict the estimate of state and covariance

$$\hat{x}_k^- = f(\hat{x}_{k-1}) + v_{k-1}$$

$$P_k^- = F_{k-1}P_{k-1}F_{k-1}^T + Q_{k-1}$$

2) Kalman gain calculation

$$K_k = P_k^- H_k^T (H_k P_k^- H_k^T + R_k)^{-1}$$

3) Data measurement, z_k

4) Update step

Update the estimate of state and covariance using the new measurement and the Kalman gain

$$\hat{x}_k = \hat{x}_k^- + K_k(z_k - H_k \hat{x}_k^-)$$

$$P_k = (1 - K_k H_k) P_k^-$$

3. Output

$$\hat{x}_k \text{ and } P_k \text{ for } t \in \{0, T\}$$

where \hat{x}_k^- and P_k^- are the priori estimate of hidden state and covariance respectively, F_{k-1} is the Jacobian of partial derivatives of f with respect to x , and H_k is the Jacobian of partial derivatives of h with respect to x .

PF provides a theoretical framework for dealing with non-linearities or non-Gaussian process observation noise (Orchard and Vachtsevanos 2009). The basic methodology approximates the conditional state probability distribution by a swarm of points called ‘particles’ each with a corresponding weight. These particles contain samples from the state-space and a set of weights representing discrete probability masses. Particles can be recursively updated given a non-linear process model, a measurement model, and a set of measurements. PF has been also widely used to predict failure prognosis for many system applications. As an example, PF combined with support vector regression was used to monitor battery state-of health and to predict the RUL of batteries (Dong *et al.* 2014). Sequential importance resampling (SIR) involves importance resampling steps to reduce the degeneracy problems of a basic particle filter, sequential importance sampling algorithm. The resampling is to eliminate particles that have small weights and extract replacement particles having large weights. Multinomial resampling scheme that uses the inverse of the cumulative density function to map independent random numbers to the events was used in this study. The recursive process of SIR filter involves prediction, data measurement, update, resampling step. The process of the SIR algorithm is presented in Algorithm 2.

Algorithm 2 The particle filter algorithm (SIR)

1. Initialization

1) Set initial sets of particles and associated weights for i in 1 to N , $x_0^i \sim p(x_0)$ and $\tilde{w}_0^i \sim p(y_0 | x_0^i)$

2) Normalize the importance weight, $w_0^i = \frac{\tilde{w}_0^i}{\sum_{j=1}^N \tilde{w}_0^j}$

2. Iteration: for t in 1 to T

1) Prediction step

Predict the estimate of particles

$$\hat{x}_k^- = f(\hat{x}_{k-1}) + v_{k-1}$$

2) Data measurement, z_k

3) Update step

Update the importance weights by computing the likelihood of each priori estimates using the new measurement, $\tilde{w}_t^i \sim p(z_t | x_t^i)$

Normalize the importance weight, $w_t^i = \frac{\tilde{w}_t^i}{\sum_{j=1}^N \tilde{w}_t^j}$

4) Resampling

Resample with replacement N particles x_t^i according to the importance weights, w_t^i

3. Output

$$\{x_t^i, w_t^i\}_{i=1}^N \text{ for } t \in \{0, T\}$$

3. Prognostic approach

This section presents a methodology for optocoupler lifetime prediction using the EKF and PF algorithms. Fig. 2 shows the overall prognosis process. In the first step, ADT was performed to collect performance degradation under accelerated stress conditions. In the second step, the EKF and PF algorithms were used to predict the lifetime of optocouplers. Finally, the performance of each prognostic algorithm was evaluated by the evaluation metrics based on accuracy and robustness.

3.1 Accelerated degradation test

Accelerated degradation test (ADT) is conducted to reduce the test time by modelling performance degradation physically or empirically (Meeker *et al.* 1999). ADT is widely used to estimate long-term performance of products and systems by understanding physical properties in degradation process. In this study, the lifetime of optocouplers was estimated before their failures by collecting the performance degradation data. ADT was performed through four stages; determination of stress conditions, determination of critical performance characteristics, experimental setup, and experiment and data collection.

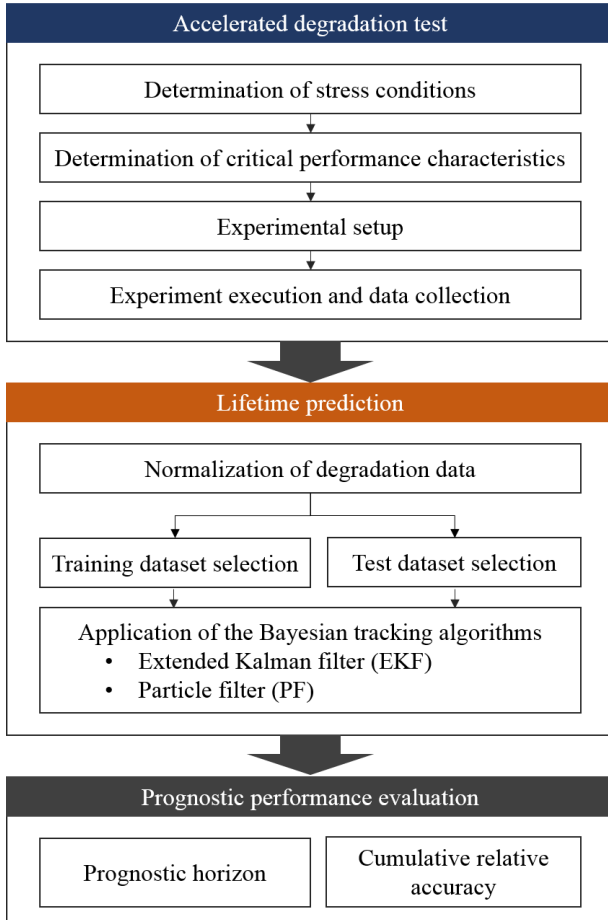


Fig. 2 Prognostic approach for optocoupler lifetime prediction

Stress conditions were identified based on the potential failure mechanisms of optocouplers as presented in the introduction. LED degradation in optocouplers was assumed to be the critical failure mechanism of digital I/O modules. The accepted model for electromigration time to failure (TTF) is a Black's equation associated with temperature and current density (Black 1969). Following Eq. (4) shows the Black's equation.

$$TTF = Aj^{-n} \exp\left(\frac{E_a}{KT}\right) \quad (4)$$

where TTF is the time to failure, A is a material dependent constant, j is the current density, n is a model parameter of 2 (Black 1974), E_a is the activation energy of 0.43eV for aluminium gallium arsenide (AlGaAs) electromigration (Mooney *et al.* 1991), K is the Boltzmann's constant, and T is temperature in Kelvin. According to the stress factors in the Black's equation, the temperature and the current density were controlled for stress acceleration. Based on the specifications from the optocoupler manufacturer datasheet, the temperature and current were controlled to 110°C and 50 mA, respectively, which were the operating margins of the optocoupler.

Critical performance characteristics are needed to explain the dominant degradation process, and can be used

to characterize product reliability (Yang, 2007). A dominant degradation phenomenon of optocouplers is current transfer ratio (CTR) reduction (Shi *et al.* 2014, Slama *et al.* 2008). CTR is a ratio of the collector current of the output side (photo sensor) to the forward current applied to the input side (LEDs) in percentage. Since CTR depends on the intensity of an LED, LED intensity reduction due to electromigration also results in CTR reduction over time. CTR is defined as shown in Eq. (5)

$$CTR = \frac{I_C}{I_F} \times 100 \quad (5)$$

where I_C is the collector current and I_F is the input forward current. To collect CTR degradation data, the collector current and the input forward current were measured.

Fig. 3 shows the schematic of the ADT that consists of test vehicles, a power supply, a data logger, a laptop, and a chamber. A test vehicle was composed of 16 optocouplers and 2 test vehicles (32 optocouplers) were used in the ADT. The power supply was controlled to supply 50 mA to optocoupler input in constant current mode, and 5 V to emitter. The inputs of all optocouplers were connected in series to drive the same input current conditions. The data logger was used to measure the input forward current and the collector current to calculate the CTR. The device under test (DUT) were Toshiba TLP291-4, which had 4 transmission paths in a single chip, and the DUT were operating in the chamber to maintain the ambient temperature at 110°C

According to (Slama *et al.* 2008), CTR barely changed at high currents, when the phototransistor in optocouplers was in saturation. It is required to identify an appropriate input forward current sensitive to CTR degradation. For CTR measurement, multiple input forward currents, ranging from 0.1 mA to 50 mA, were swept for 0.25 second every 4 hour, and during the rest of the ADT, the input forward current was maintained at 50 mA.

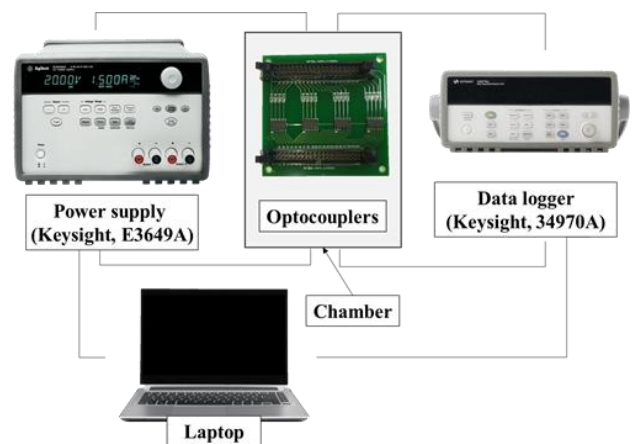


Fig. 3 Schematic of the accelerated degradation test

3.2 Lifetime prediction

The lifetime prediction procedure included pre-processing of the CTR, estimation of the CTR degradation, lifetime prediction of optocouplers using EKF and PF, and comparison of the prediction performance.

Firstly, the CTR was normalized by dividing the CTR by the initial CTR at time zero. It was required to determine the failure of optocouplers, because a 50% degradation from the initial CTR is considered to failure. Siemens, for example, defined the end of life of optocouplers as when the CTR drops to 50%. The normalized CTR is defined as shown in Eq. (6)

$$\text{normalized CTR (\%)} = \frac{CTR_t}{CTR_0} \times 100 \quad (6)$$

where CTR_t is the CTR at time t and CTR_0 is the initial CTR.

Normalized degradation data from 32 optocouplers was divided into a training dataset a test dataset. The training dataset was a set of examples used to fit the parameters of the degradation model in the lifetime prediction, and the test dataset was used to assess the performance of the prediction algorithm specified using the training dataset. 16 optocouplers were randomly selected to be the training dataset to determine the initial state, covariance, and noise through model fitting. The remaining 16 optocouplers were used as the test datasets to evaluate the lifetime prediction performance.

Next, the degradation of normalized CTR was estimated using EKF and PF to deal with the nonlinear degradation behaviour. The degradation trajectory of CTR was assumed to follow an exponential curve because CTR degradation is occurred from the LED lumen degradation. According to IES TM-21-11, long term lumen maintenance of LED light sources, LED aging behaviour is suggested to be described and extrapolated by using an exponential function. Accordingly, the measurement model is defined as shown in Eq. (7).

$$z_k = A_k \times \exp(-B_k \times t_k) + n_k \quad (7)$$

where z_k is the normalized CTR, A_k and B_k are measurement model parameters, t_k is time, n_k is measurement noise, and k is the measurement cycle.

The parameters of the measurement model were determined to be the states of the nonlinear state-space model. The state model is defined as shown in Eqs. (8)-(10).

$$\mathbf{x}_k = \begin{bmatrix} A_k \\ B_k \end{bmatrix} \quad (8)$$

$$A_k = A_{k-1} + v_{k-1}^A \quad v_{k-1}^A \sim N(\mathbf{0}, Q_v^A) \quad (9)$$

$$B_k = B_{k-1} + v_{k-1}^B \quad v_{k-1}^B \sim N(\mathbf{0}, Q_v^B) \quad (10)$$

where \mathbf{x}_k is the state vector, v_k is the state noise, and Q_k is the covariance of state noise.

To begin the lifetime prediction using EKF and PF

algorithms, an initial state vector and noise of state model were needed. The initial state vector was determined by the exponential fitting using the training dataset. The covariance of the fitted model parameters was also used to determine the covariance of state noise. On the other hand, the measurement noise was assumed to be Gaussian and was determined based on the standard derivation of the training dataset measurements. In SIR filter, the likelihood function was normal distribution and the initial distribution of particles were assumed to be uniform.

3.3 Performance evaluation

The lifetime prediction performance was evaluated by prognostic horizon (PH) and cumulative relative accuracy (CRA) (Saxena *et al.* 2008). PH evaluates the difference between the first time of prediction and the end of life. The allowable performance boundary was determined to be 10% error bound of the initial true RUL around the true RUL. In PH evaluation, the longer PH implies the earlier convergence to the true RUL range. RA is defined as a measure of error in RUL prediction relative to the true RUL, described by Eq. (11).

$$RA_\lambda = 1 - \frac{|r_*(i_\lambda) - \langle r^l(i_\lambda) \rangle|}{r_*(i_\lambda)} \quad (11)$$

where λ is the time window modifier, l is the index for l^{th} device under test, $r_*(i_\lambda)$ is the truth RUL at time index i_λ , and $\langle r^l(i_\lambda) \rangle$ is an appropriate point estimate of the predicted RUL distribution at that time. CRA evaluates the relative accuracy of RUL prediction at multiple time instances to estimate the overall prediction performance, as shown in equation.

$$CRA_\lambda = \frac{1}{|l_\lambda|} \sum_{i \in l_\lambda} w(r(i)) RA_\lambda \quad (12)$$

where $w(r(i))$ is a weight factor as a function of the RUL at all the time indices, l_λ is the set of all time indexes when a prediction was made. It is common to give more weight to RA evaluated at times closer to the end of life (EOL) since good performance close to the EOL is important for decision making. In this study, the RA closer to the EOL was exponentially weighted.

4. Results

The failure was defined to be the time at which CTR drops to 80% of the initial value due to the limited test time. The CTR degradation trajectory was analyzed to identify the most sensitive input forward current to CTR degradation.

4.1 The input forward current condition for degradation data measurement

The degradation rates of the normalized CTR varied according to each input forward current. Fig. 4 shows the normalized CTR trajectories over time with their standard deviations when the input forward current was from 0.1 mA to 50 mA.

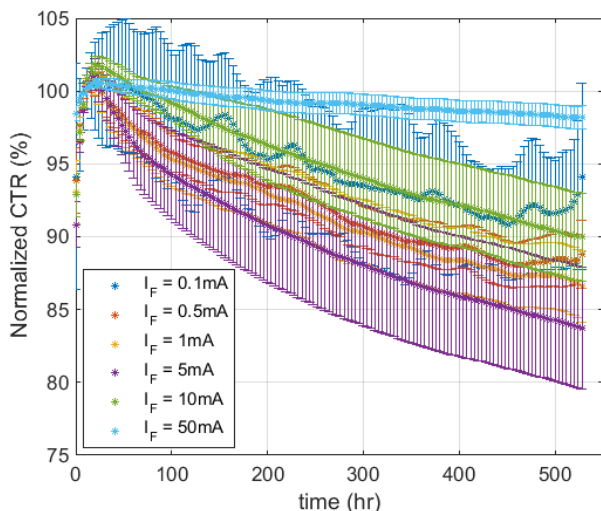


Fig. 4 CTR degradation in different input forward current conditions

The normalized CTR showed some fluctuations when the input forward current was 0.1 mA because of the resolution limit of the measuring equipment. The CTR of all the training samples was higher than 95% even after 500 hours of testing. It might be due to saturation mode operation of the optocoupler when the input forward current was over 10 mA. When the input forward current is 5 mA, the CTR showed the highest degradation rate. 5 mA was consistent with the input forward current condition of the most sensitive CTR provided by the manufacturer of optocouplers. Thus, 5 mA was used for input forward current condition for lifetime prediction.

4.2 Lifetime prediction

The measurement data from 0 to 12 hours, during which the CTR was increasing, was used to obtain the initial states which were the parameters of degradation model by exponential model fitting. Starting from the initial states of degradation model, CTR degradation until 200 hours was estimated by recursive estimation using the measurement. Fig. 5 shows the true normalized CTR degradation and the CTR estimated by EKF and PF of a sample, respectively. The estimation curve with PF followed the true normalized CTR during the entire estimation period. However, the estimation curve with EKF showed larger residuals than the result with PF in the early estimation period. The root mean square errors (RMSEs) of EKF and PF estimation of the sample were calculated to be 1.08 and 0.09, respectively. RMSE of EKF estimation for every test samples was higher than RMSE of PF estimation; and, the mean RMSEs of EKF and PF estimation were 1.16 and 0.1 respectively.

The CTR degradation was predicted at 200 hours using EKF and PF. Fig. 6 shows the CTR degradation prediction. The predicted TTFs with EKF and PF were 384 and 368 hours, respectively, which was earlier than the true TTF. The prediction error of EKF was lower than that of PF.

Fig. 7 shows the results of EKF and PF prediction performance evaluation. Fig. 8 shows the evaluation results for all the test samples. As shown in Fig. 7(a), EKF exhibited a longer PH than PF. RUL prediction by EKF converged within the accuracy boundary 404 hours prior to the failure. On the other hand, time to convergence of PF algorithm was 192 hours before the failure. Fig. 7(b) shows the PH results across all the test samples. The CRAs of EKF and PF were calculated to be 0.116 and 0.0113, respectively.

4.3 Real lifetime prediction

To compute the expected field lifetime from the accelerated degradation test, an acceleration factor was calculated based on the Black's equation. Acceleration factor (AF) can be calculated by referring to the ratio of the lifetime between use conditions and accelerated test conditions. Eq. (13) shows the AF calculation.

$$AF = \frac{TTF_{use}}{TTF_{acc}} = \left(\frac{j_{acc}}{j_{use}}\right)^n \exp\left(\frac{E_a}{K} \left\{\frac{1}{T_{use}} - \frac{1}{T_{acc}}\right\}\right) \quad (13)$$

where TTF_{use} is the time to failure in use condition, TTF_{acc} is the time to failure in accelerated test condition, j_{acc} is the current density in accelerated condition, j_{use} is the current density in use condition, T_{use} is the operating temperature in use condition, and T_{acc} is the operating temperature in accelerated condition. As an example, when an ambient temperature and an operating current are 59°C and 20 mA respectively, AF is calculated to be 184.

5. Conclusions

This paper presented a prognostic approach of digital I/O modules by identifying the critical components and predicting the RUL of the critical components using EKF and PF. Critical items in the digital I/O modules were identified to be optocouplers in terms of the risk of failures. During the lifetime, optocouplers deteriorated due to electromigration on LEDs resulting from thermal and electrical stress. As a result of experimental verification, both EKF and PF showed accurate and robust prediction of RUL.

Our future works on this topic include continuing accelerated life tests of optocouplers to obtain long term CTR degradation data. In addition, the digital I/O modules will be under accelerated life tests to compare the lifetime of digital I/O modules and optocouplers.

Acknowledgments

This research was supported by Basic Science Research Program through the National Research Foundation of Korea (NRF) funded by the Ministry of Education (NRF-2017R1D1A1B03028604).

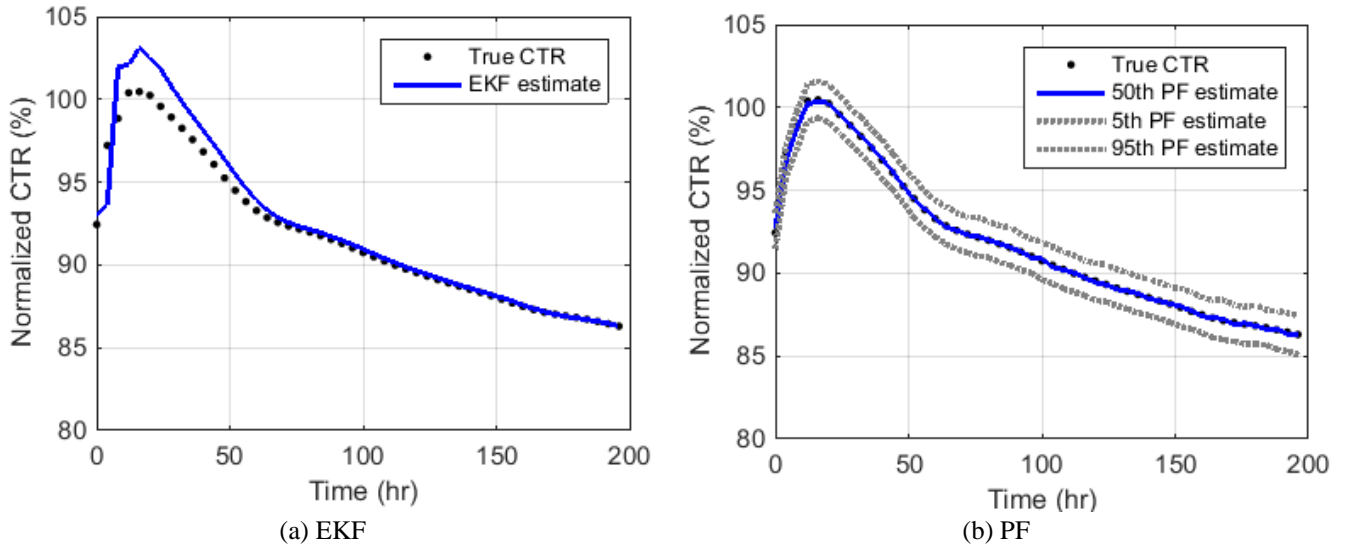


Fig. 5 The CTR degradation estimation by using EKF and PF

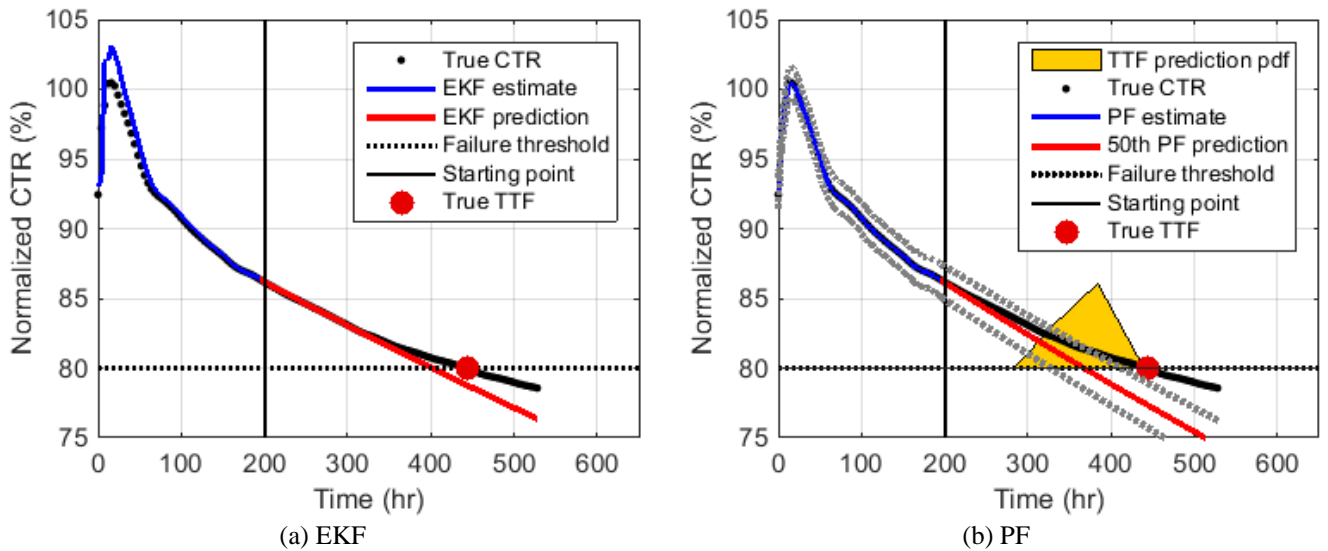


Fig. 6 The CTR degradation prediction by using EKF and PF

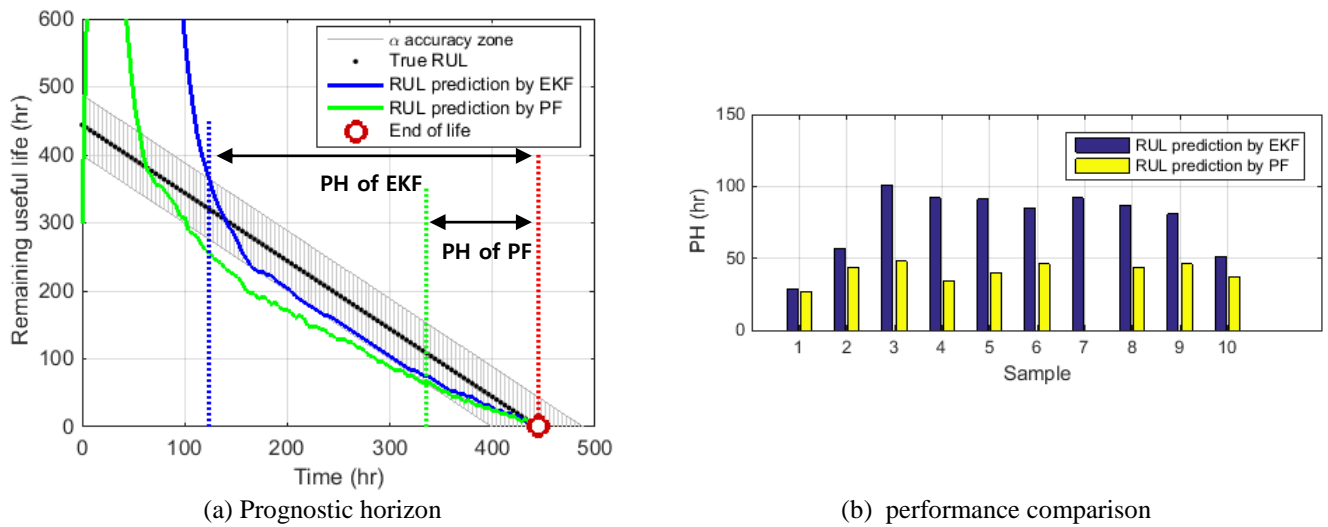


Fig. 7 The RUL prediction performance of EKF and PF

References

- Authen, S. and Holmberg, J.E. (2012), "Reliability analysis of digital systems in a probabilistic risk analysis for nuclear power plants", *Nuclear Eng. Technol.*, **44**(5), 471-482.
- Black, J.R. (1969), "Electromigration failure modes in aluminum metallization for semiconductor devices", *Proceedings of the IEEE*, **57**(9), 1587-1594.
- Black, J.R. (1974), "Physics of electromigration", Reliability Physics Symposium, Las Vegas, NV.
- Brown, K. (2004), Metal Oxide Varistor Degradation, International Association Electrical Inspectors.
- Chiu, T.C., Zeng, K., Stierman, R., Edwards, D. and Ano, K. (2004), "Effect of thermal aging on board level drop reliability for Pb-free BGA packages", *Proceedings of the 54th Electronic Components and Technology Conference*, La Vegas, NV: IEEE.
- Chu, T.L., Martinez-Guridi, G., Yue, M., Lehner, J. and Samanta, P. (2008), Traditional Probabilistic Risk Assessment Methods for Digital Systems, Washington DC: United States Nuclear Regulatory Commission.
- Chu, T.L., Yeu, M., Martinez-Guridi, G., Mernick, K., Lehner, J. and Kuritzky, A. (2009), Modeling a Digital Feedwater Control System Using Traditional Probabilistic Risk Assessment Methods, NY: United States Nuclear Regulatory Commission.
- Dong, H., Jin, X., Lou, Y. and Wang, C. (2014), "Lithium-ion battery state of health monitoring and remaining useful life prediction based on support vector regression-particle filter", *J. Power Sources*, **271**, 114-123.
- Doucet, A., de Freitas, N. and Gordon, N. (2001), An introduction to Sequential Monte Carlo methods, Springer-Verlag.
- Feng, Z., Wen-fang, X. and Liu, X. (2011), "Overview of nonlinear bayesian filtering algorithm", *Procedia Eng.*, **15**, 489-495.
- Ginsberg, D., Fritzen, C. and Loffeld, O. (2018), "Sparsity-constrained Extended kalman filter concept for damage localization and identification in mechanical structures", *Smart Struct. Syst.*, **21**(6), 741-749.
- IEEE Standards Association (2006), IEEE Std 650-2006, IEEE Standard for Qualification of Class 1E Static Battery Chargers and Inverters for Nuclear Power Generating Stations.
- Illuminating Engineering Society (2011), IES TM-21-11, Projecting Long Term Lumen Maintenance of LED Light Sources.
- International Electrotechnical Commission (2006), Analysis techniques for system reliability - Procedure for failure mode and effects analysis (FMEA). IEC 60812.
- Kulkarni, C., Biswas, G. and Koutsoukos, X. (2009), "A prognosis case study for electrolytic capacitor degradation in DC-DC converters", *Proceedings of the Annual Conference of the Prognostics and Health Management Society*.
- Lall, P., Lowe, R. and Geobel, K. (2011), "Extended Kalman Filter models and resistance spectroscopy for prognostication and health monitoring of leadfree electronics under vibration", *Prognostics and Health Management*, 1-12, Montreal: IEEE.
- Lee, S.J., Jung, W. and Yang, J. (2016), PSA Model with Consideration of The Effect of Fault-tolerant Techniques in Digital I&C Systems, *Annls of Nuclear Energy*, 375-384.
- Meeker, W.Q., Escobar, L.A. and Lu, J.C. (1999), Accelerated Degradation Tests: Modeling and Analysis, Statistics Preprints, 2.
- Mohammadian, H.S., Aiiit-Kadi, D. and Routhier, F. (2010), "Quantitative accelerated degradation testing: Practical approaches", *Reliab. Eng. Syst. Safe.*, **95**(2), 149-159.
- Mooney, P.M., Theis, T.N. and Calleja, E. (1991), "Effect of local alloy disorder on the emission kinetics of deep donors (DX centers) in AlxGa1-xAs", *J. Electron. Mater.*, **20**(1), 23-33.
- National Instruments (2015), Digital I/O for test, control, and design. Retrieved from <http://www.ni.com>
- Orchard, M.E. and Vachtsevanos, G.J. (2009), "A particle-filtering approach for on-line fault diagnosis and failure prognosis", *Transactions of the Institute of Measurement and Control*, 221-246.
- Shi, Z., Lu, Y., Chen, Y. and Feng, J. (2014), "The real-time fault diagnosis of optocoupler in switching mode power supply", *Proceedings of the International Conference on Reliability, Maintainability and Safety*, Guangzhou.
- Singleton, R.K., Strangas, E.G. and Aviyente, S. (2015), "Extended kalman filtering for remaining-useful-life estimation of bearings", *T. Ind. Electron.*, **62**(3), 1781-1790.
- Slama, J., Helali, S., Lahyani, A., Louati, K., Venet, P. and Rojat, G. (2008), "Study and modelling of optocouplers ageing", *J. Autom. Syst. Eng.*, 2(3).
- Terejanu, G.A. (2007), Extended Kalman Filter Tutorial, Buffalo, NY, USA.
- Yang, G. (2007), Degradation testing and analysis, In G. Yang, Life Cycle Reliability Engineering, John Wiley & Sons, Inc.
- Yoshida, I. and Akiyama, M. (2013), "Particle filter for model updating and reliability estimation of existing structures", *Smart Struct. Syst.*, **11**(1), 103-122.